Development and research of mathematical model of 3D track detector for nanosatellite

O.V. Phylonin[1], K.S. Nasonov[1]

[1]Samara National Research University, Moskovskoe Shosse 34A, Samara, Russia, 443086

Abstract. The article provides information about ionizing radiation as a factor of outer space. The authors have developed and researched a 3D track detector of radiation for nano-satellite. The layout and principal device of the detector are considered. The detection and information abilities of the developed device are estimated. The modeling of the main processes occurring in the detector is carried out by methods of mathematical modelling.

1. Introduction

Every year space technology becomes more and more functional. The devices acquire new functions, increase productivity, energy efficiency, there is a tendency to miniaturization, manifested in the growth of the number of nanosatellites capable of performing more and more serious tasks from year to year. This is mainly due to the development of microelectronic systems, reduced process technology, increasing the number of components per unit area, but at the same time, increases the radiation vulnerability of the element base. This is due to the presence of one of the main factors of outer space – ionizing cosmic radiation of different origin and different energy spectra. The study of the impact of ionizing radiation on microelectronic systems of nanosatellite is especially important, because often such devices do not have a specialized, radiation-resistant element base. However, in addition to studying directly the effects of radiation, the actual and the objective of the study and clarification of data on the radiation parameters, the data about the energies of the particles, qualitative and quantitative distribution, determination of flows. To solve the latter problem, many detectors are used for both space and earth applications [1].

Ionizing radiation is usually classified according to the energy values, from this point of view, and based on the data on the origin of the particles, cosmic radiation is divided into the following groups:

1) Galactic cosmic rays $\sim 10^{18}$ eV
2) Metagalactic cosmic rays $>10^{18}$ eV
3) Solar cosmic rays $\sim 10^{10}$ eV
4) Abnormal cosmic rays $\sim 10^{9}$ eV
5) Abnormal cosmic rays $\sim 10^{5}$ eV

However, hazard assessment based only on the energy of the flow is not fully correct. An important characteristic of the flow in addition to energy is its value, defined as $(cm^{2}*MeV)^{-1}$. From this point of view, the standard particle energy for estimating radiation defects is 100 keV, the particle flux with such energy is the highest for the heights of the order of 500 km – $1*10^{15}$ for electrons and $1*10^{13}$ for protons.

Ionizing radiation can be a source of data distortion during the experiments. Clearly, this effect can be seen from the comparative photos in the figure, Fig. 1. For comparison, the photos before the solar

flare and after are given. As you can see, the image on the right is very noisy, which is caused by increased 4 times the flow of charged particles.

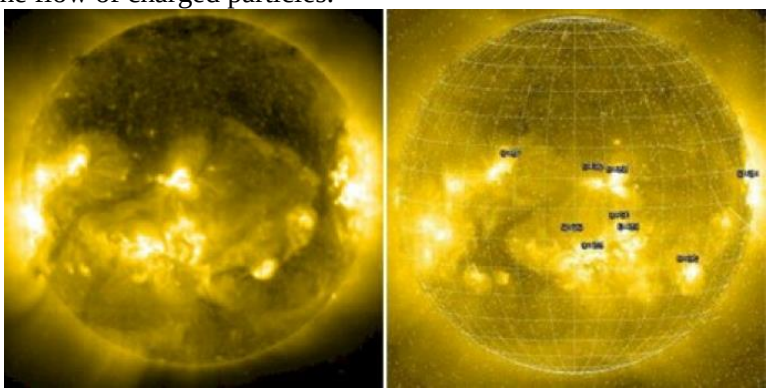

Figure 1. Photographs of the Sun taken by EIT instrument (SOHO).

2. Multi-wire 3D track detector for nanosatellite

Samara University has developed a multi-wire 3D track detector for nanosatellite. The proposed device is a payload module made in the classical format for nanosatellites CubeSat, occupying one unit, 1U. A sketch of the developed detector is shown in the figure, Fig. 2.

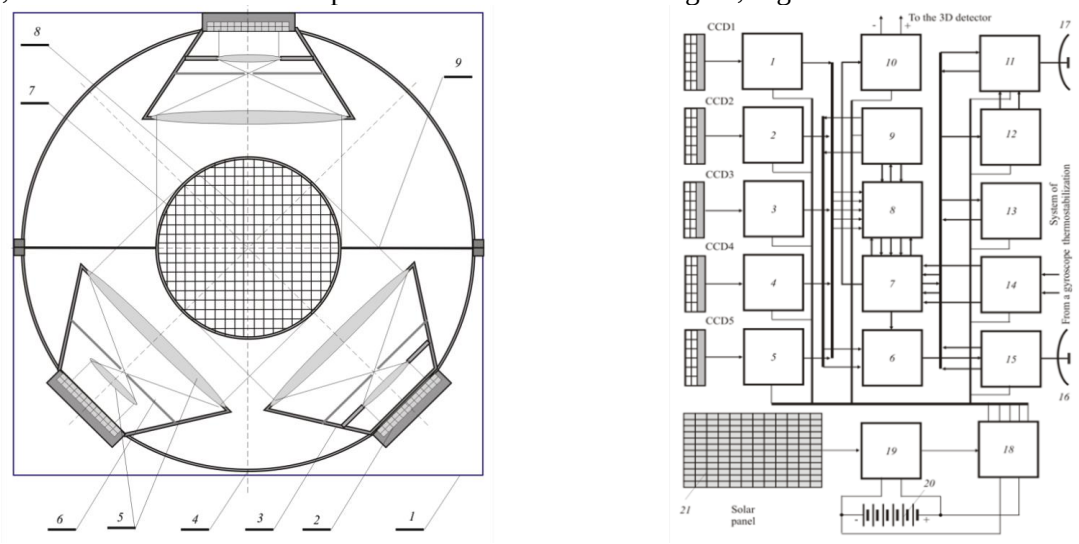

a) b)

Figure 2. Sketch of multi-wire detector for nanosatellite (a), block diagram of the detector (b).

The detector includes the following components according to the designations in the figure, Fig. 2 (A):

1) The module housing
2) CCD-matrix
3) Case optical of the Registrar
4) The body of the detector
5) Lens
6) Aperture
7) Transparent sphere (d = 40 mm)
8) The working volume of the detector
9) Introductory contacts

Multi-wire detectors of ionizing radiation have a number of advantages over ionization, Geiger counters, scintillation, semiconductor detectors and others. Intensively developed gas electronic multipliers on a plastic basis due to the cellular structure and high gain make it easy to implement the spatial resolution of the X -, Y-coordinates. In addition, due to the separation of the electronic

component of the avalanche, they can provide high spatial resolution and Z – coordinate. Structurally, a multi-wire proportional chamber (MPC) is a system of many thin (10 μm) parallel wires located in the same plane and being anodes that are in the gas volume between two flat cathodes parallel to each other and the anode (solid or wire). In a typical case, the anode wires are removed from each other by 2 mm and from the cathodes at a distance of 8 mm. the potential Difference between the anode and the cathode is several kV. Such MPC parameters provide gas amplification ($10^4 \div 10^5$) and proportionality of the signal amplitude of the energy left by the particle in the gas volume. Thus, the MPC is essentially a system of multiplied proportional counters. With the passage of a charged particle through the MPC, formed along the particle track free electrons give rise to avalanches, arriving on the anode wire closest to that of the primary electrons. The electronics register the signal from each wire. Thus, the incoming signals indicate the position (coordinates) of the particle in the MPC. In order to obtain three-dimensional coordinates of a particle in a large volume, systems of tens of MPC with an area of up to 10 m^2 are used, which are arranged in parallel one after another, with a total number of tens of thousands of wires, and the wires of two neighboring MPC are stretched mutually perpendicular. Typical spatial resolution of modern MPC (0.05÷0.3) mm. Temporal resolution is several nanoseconds. The energy resolution of the proportional chamber is 10%. It should be noted that in multi – wire track detectors with an increase in voltage, with this gas mixture, various modes can be implemented: ionization, proportional, self-quenching, Geiger-Muller mode. The type of mode in which proportional detectors pass after the proportional mode is determined by the composition and pressure of the gas, geometric parameters, the magnitude of the voltage between the electrodes [2].

The most important task in the field of research of influence of a solar wind on a condition of an ionosphere, in particular F – layer is constant monitoring of its parameters. Tasks of this kind can be successfully solved with the help of NS. Recall that most microsatellites and NS are placed in low orbits (250 ÷ 600) km. Samara University has developed a small-sized 3D track detector to analyze the parameters of the solar wind, as well as particles of cosmic rays captured by the magnetosphere. Given that the solar wind consists mainly of electrons, protons and helium nuclei (alpha particles); the nuclei of other elements and non-ionized particles (electrically neutral) are contained in a very small amount, as a detecting module was proposed gas detector, multi-wire type. The detecting head is made in the form of a ball with a diameter of 40 mm, contains 40 mutually orthogonal layers of wires with a diameter of 0.01 mm, the distance between adjacent layers of 1 mm. The wires are stretched on a sphere of 7 of transparent optical plastic, 0.1 mm thick. The layers of one direction applied to either the constant potential (500÷2000), or an alternating pulse voltage in the same range of amplitudes, the frequency of the square wave is 20 kHz via the contacts 9. The inert gases Ar, Ne in equal concentrations are selected as the gas medium, the pressure in the chamber is (0,1,...,0,2) bar. The principle of operation of this track detector is as follows. If the incident particle, proton, alpha particle, electron, gamma quantum produces ionization of atoms in the zone of intersection of wires, where an electric field of high heterogeneity is created, then an avalanche process develops in the zone of the wire, accompanied by a glow in the optical region. In the orbits of the NS, the flux densities of, for example, neutrons born by the Sun are $2{,}4\times10^8$ $cm^{-2}s^{-1}$, which can lead to intense illumination of the entire volume of the detector. To eliminate this effect, the detector mode control module should reduce the voltage applied to the electrodes. In this system the tomographic method of processing of initial data which essence is reduced to the following is applied [3]: Optical radiation induced in the ball region 8 of the detector is recorded as a two-dimensional projection according to sphere tangential geometry. This system uses five optical recorders. Each logger has a high-speed CCD matrix based on the digital microscope Levenhuk DTX 30, forming a two-dimensional image in jpeg format (640x480) pixels. The image from the luminous objects in the ball zone of the detector using lenses 5 and aperture 6 is projected onto the matrix according to the orthogonal projection geometry. The lenses, diaphragm and matrix are placed in the housing 3, and the optical recorders themselves are fixed in the spherical housing of the detector 4 made of carbon fiber, 0.6 mm thick. The diameter of the detector body is 92 mm, which allows it to be placed in one module of HC 1 of 1U CubeSat format.

Figure 2 (B) shows a block diagram of the control modules of the detector operation modes, data pre-processing systems and their transmission to the MCC, thermal stabilization systems and NS

orientation. Since the processes of generation of tracks quite fleeting – of the order of microseconds, the optical detectors shall simultaneously forming image frames, it is possible to implement if each CCD 1,...,5 the matrix is driven by its "own" microprocessor 1,...,5. Data flows from these microprocessors are fed into switch 8, which is connected to the on-Board microcomputer 5 and the pre-processing microprocessor 9. Since the capabilities of the NS radio channels are extremely limited, the task of the microprocessor 9 is to create a format of 128×128 elements from the 640×480 format and transfer data from the Cartesian grid to the polar one. Thus, 5×128×(128) one-dimensional arrays of data are formed, which are transmitted through the code generator 12 via the transceiver 11 via a separate channel to the MCC. For the effective operation of this detector requires a certain orientation of the NS in space. The orientation correction is carried out by means of miniature ion engines according to the data of a three-axis gyroscope connected through the control unit 14 to the onboard microcomputer 7.

3. Simulation of the detector field and tracing the motion of charged particles in the detector field

To solve the problem of tracing the motion of particles in the detector field, a model of the detector was built. In contrast to the supposed real design of the detector, an assumption was made about the geometric parameters of the detector, namely, the model describes a cubic detector. This assumption was mainly made to simplify the construction of the grid at the borders, as well as to simplify the solution of the problem. It should be noted that despite the assumption, the physics of the described process is unchanged. The parameters of the detector:

1) the dimensions of the active area of the detector – 12x12x12 mm;
2) the Number of wires – 10 pieces
3) the Spatial pitch of the wires is 1 mm
4) wire Thickness – 0.1 mm
5) the section profile of the wire – square
6) Material of wire – copper
7) is Applied to the anode voltage 1 kV
8) the working substance – argon
9) working fluid Pressure-0.1 bar

The wires have a serpentine shape. The spatial configuration of the wires is shown in the figure, Fig. 3.

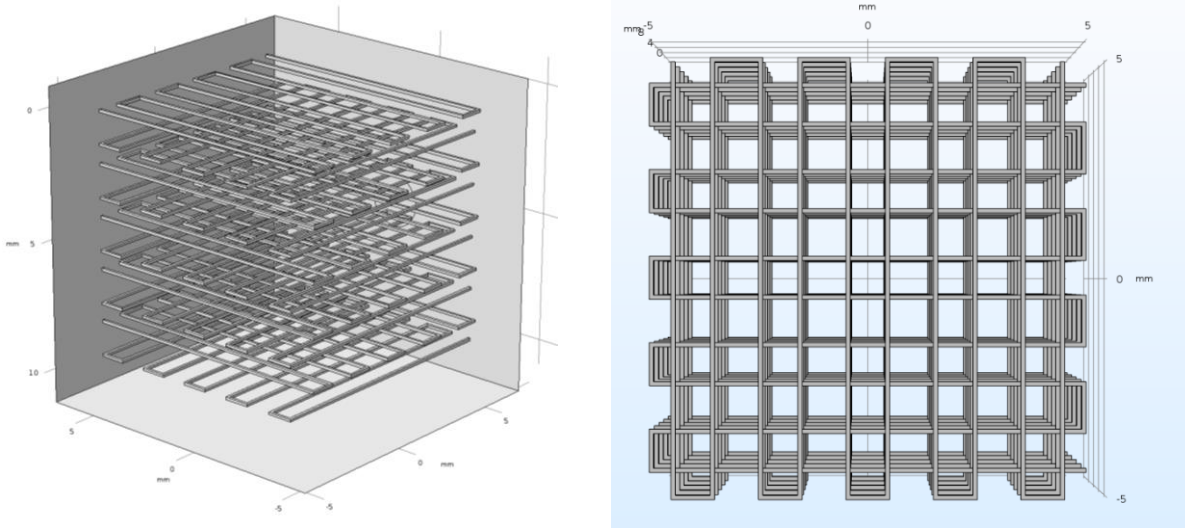

Figure 3. Spatial arrangement of wires in the working volume of the detector.

The field strength of the detector is described by the known ratio, E= - φ φ. Was built the line tension detector and an equipotential surface, the drawing, Fig. 4.

Conditions of detector field modeling:

1) The voltage at the anode – 1000 Volts

2) The cathode is grounded
3) The number of lines of field intensity displayed at the same time-2000

Then, using the emittance, the trace of particles in the detector field was carried out. The trace parameters of electrons and protons:

1) The charge of a proton is $1.6*10^{-19}$ C
2) The mass of a proton is $1.6*10^{-27}$ kg
3) The electron charge is $-1.6*10^{-19}$ C
4) The electron mass is $9.1*10^{-34}$ kg
5) The initial energy of the electrons and protons of 0.1 MeV
6) The number of simulated particles at a time – 20 pieces

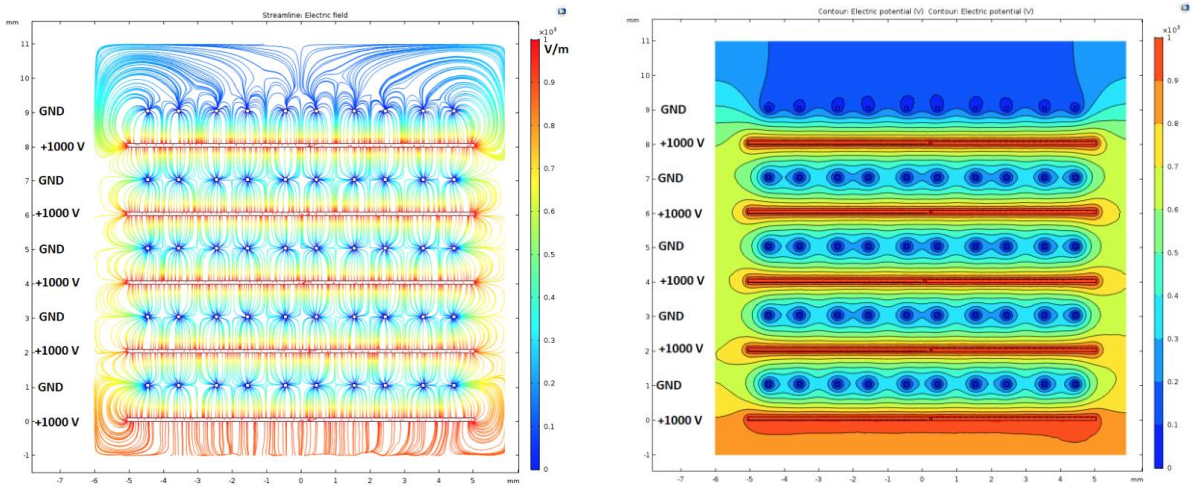

a) b)

Figure 4. The line tension detector (a); equipotential surface of the detector (b) Simulation results for electrons are shown in Fig. 5 (a), for protons in the figure, Fig. 5 (b).

As can be seen from the simulation results, the trajectories of protons and electrons at equal initial energies undergo changes strikingly different from each other. These differences are due to the fact that the masses of the particles are significantly different from each other, which means that protons are more inert and the deviation of protons requires a significantly greater force from the field. These data allow us to conclude that the further solution of the problem of determining the variety of detected particles is greatly simplified.

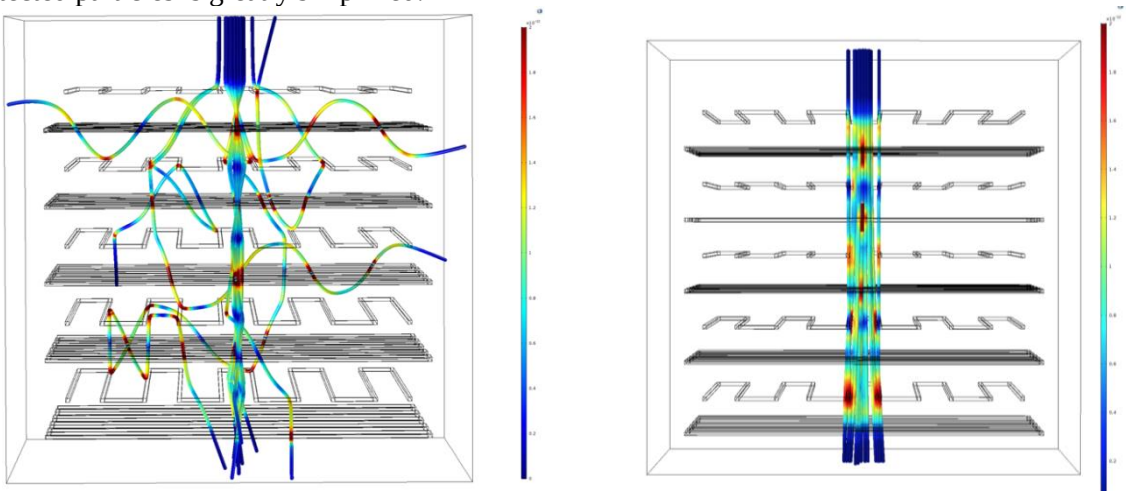

a) b)

Figure 5. Tracing the flow of electrons in the detector field (a); tracing the flow of protons (b).

4. Modeling of ionization losses of proton and electron beams

The Joe-Luo model, formula (1), is used to calculate the ionization losses by the electron beam: [4]

$$S_{jl}(Z,E) = 785\frac{Z\rho}{AE}\ln\left(\frac{1.166E}{d_1 Z} + d_2\right), \quad (1)$$

where: S_{jl} is the braking energy loss of a particle per unit path length in the target material (eV/Å); Z-sequence number of the element; E-energy in electron volts; ρ is the density of the target; A – atomic mass of the target; d_1, d_2 – coefficients specific to each element (reference data).

The Mott (2) formula is used to calculate the scattering cross section):

$$\left(\frac{d\sigma}{d\Omega}\right)_{Mott} = \frac{\alpha^2}{4E^2 sin^4\theta/2} cos^2\frac{\theta}{2}, \quad (2)$$

where $\left(\frac{d\sigma}{d\Omega}\right)_{Mott}$ – the scattering cross section of the electron beam; $\frac{\alpha^2}{4E^2 sin^4\theta/2}$ – adjusted Rutherford formula for elastic electron scattering; $cos^2\frac{\theta}{2}$ – reflects the overlap of the electron wave functions at the initial and final moments of time.

The simulation was performed with the following initial parameters:

1) Energy of the electron beam is 100 Kev
2) Geometrical dimensions of the bombarded region – 12x12x12 mm
3) the Number of simulated particles – 1000
4) the Number of simultaneously displayed trajectories – 200
5) atoms of the target (the working body of the detector).
6) the Density of the working fluid – 0.00016 gr/cm^3
7) the Angle of incidence is 90º
8) electron beam Diameter – 1 nm
9) the Occurrence of secondary radiation-no

Simulation results are shown in figure, Fig. 6.

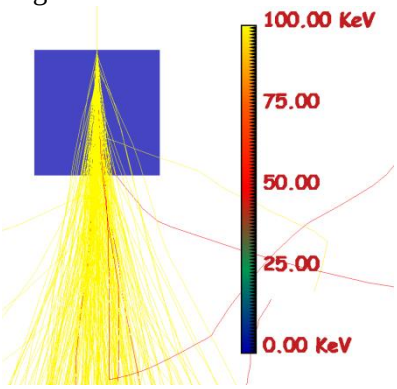

Figure 6. Electron range in the working volume of the detector.

The ionization losses of the proton beam were estimated using the Kinchin–Pisa model (3). This model has 2 main limitations:

1) there is no particle annihilation;
2) the collision is elastic;

The number of displaced atoms is determined as follows (4) [5].

$$N_d(P) = \begin{cases} = 0 \\ = 1 \\ = \frac{0{,}8E_d(P)}{2E_d} \end{cases} \quad \begin{cases} 0 < P < E_d \\ E_d < P < 2{,}5E_d \\ 2{,}5E_d < P < P_{max} \end{cases}, \quad (3)$$

$$P_{max} = \frac{E(4m_1m_2)}{(m_1+m_2)}, \quad (4)$$

where: Ed is the threshold energy of atomic displacement; Pmax is the maximum energy that can be transmitted by an incident particle with energy E and mass m1 to target atoms with mass m2; Nd(P) is the number of offsets; Ed (P) – damage energy, i.e. energy dissipated in nuclear collisions.

Conditions of simulation:

1) Buffer zone to detector – 1 mm

2) Buffer zone after the detector – 1 mm
3) the Number of particles in the beam – 1000
4) the Number of displayed trajectories – 1000
5) the working substance – Ar
6) the Density of Ar – 0.00016 gr/cm^3
7) the energy of the particles in the beam is 100 Kev
8) the Geometric dimensions of the bombarded region – 12x12x12 mm
9) the diameter of the proton beam – 1 nm
10) the Angle of incidence is 90º
11) the Occurrence of secondary radiation – no

The buffer zone was chosen for clarity, it is an absolute vacuum and does not affect the mileage of the particles. The trajectories of ionizing particles are shown in Fig. 7.

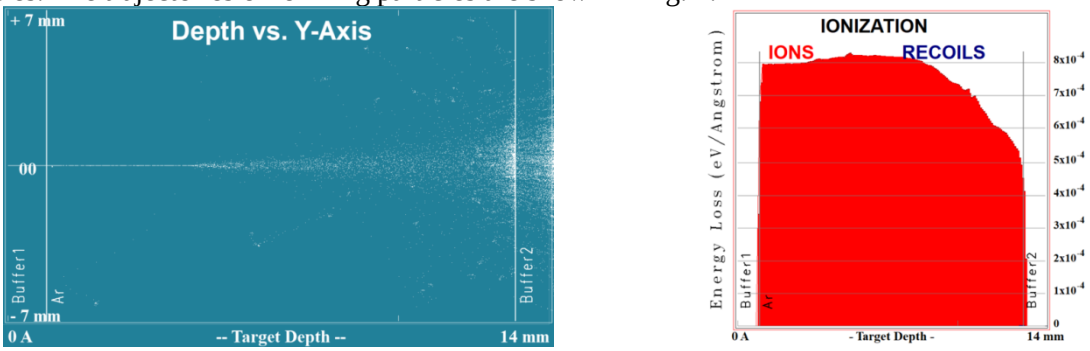

a) b)

Figure 7. Proton trajectories in the detector working volume (a); specific ionization losses of protons in the detector field (b).

As can be seen from figure 7 (A), collisions leading to ionization slightly deflect protons, but nevertheless, they continue to maintain the main vector of motion, which indicates a slight effect of ionization on the energy of the particles themselves, this is also evidenced by figure 7 (B), which shows the specific ionization losses – per unit of length, eV/Angstrom. As you can see, the highest ionization value is 8*10^{-4} eV, or 80 millieV, which is 12 orders of magnitude different from the initial beam energy. It can be concluded that this indicator is conditionally good, since it allows to restore the initial value of the energy of the ionizing particle up to an order of magnitude.

5. Conclusion

The study suggests a potentially high detection and information capacity of multi-wire 3D track detectors based on the phenomenon of gas discharge. An integrated approach to radiation detection and processing of the results by low – competition optical tomography makes it possible to Refine the data on ionizing radiation at altitudes corresponding to the near space-the area of operation of nanosatellites. Multiple groups of such devices allow us to make estimates of the state of the radiation situation in real time, and thus make adjustments to the experiments, as well as to take into account the radiation data in the design of new components of the element base of spacecraft.

6. References

[1] Panasyuk, M.I. Project of the Department of General and Nuclear Physics, Faculty of Physics, MSU: Cosmic Rays [Electronic resource]. – Access mode: http://nuclphys.sinp.msu.ru/pilgrims/cr04.htm. (30.04.2018).
[2] Rayzer, Yu.P. Gas Discharge Physics. – M.: Nauka, 1992. – 536 p.
[3] Phylonin, O.V. Inverse ill-posed problems in space research. – Samara: SSC RAS, 2014. – 478 p.
[4] Malerba, L. Nuclear Science // Primary Radiation Damage in Materials. – 2015. – Vol. 9. – P. 86.
[5] Li, Y.G. Applications of Monte Carlo Method in Science and Engineering // Monte Carlo Simulation of SEM and SAM Images. – 2011. – P. 232-251.